International Journal of Applied Engineering Research ISSN 0973-4562 Volume 13, Number 19 (2018) pp. 14079-14086

24-Hour Prediction of Solar Irradiance for a Photovoltaic Microgrid Using Neural Networks

Mauricio Mauledoux
Assistant Professor, Department of Mechatronics Engineering, Militar Nueva Granada University
Bogotá, Colombia, mauricio.mauledoux@unimilitar.edu.co

Vladimir P Jiménez
Auxiliary Professor, Department of Mechatronics Engineering, Militar Nueva Granada University
Bogotá, Colombia, vladimir.prada@unimilitar.edu.co

Edilberto Mejía Ruda
Auxiliary Professor, Department of Biomedical Engineering, Militar Nueva Granada University
Bogotá, Colombia, edilberto.mejia@unimilitar.edu.co

Oscar I. Caldas
Auxiliary Professor, Department of Industrial Engineering, Militar Nueva Granada University
Bogotá, Colombia, oscar.caldas@unimilitar.edu.co

Oscar F. Avilés S
Titular Professor, Department of Mechatronics Engineering, Militar Nueva Granada University
Bogotá, Colombia, oscar.aviles@unimilitar.edu.co

Abstract

This paper presents the implementation of Neural Network Fitting (NNF) to predict the energy of Photovoltaic (PV) modules. This prediction is made to properly manage energy charging to a battery bank. The PV modules and the battery bank (storage) are part of a micro grid along with other backup power sources such as wind turbines and the Colombian electric grid, to light two tennis courts at the sports complex of the Militar Nueva Granada University, that require up to 3 kW to operate. Therefore, this paper begins with an introduction regarding the purpose of this work and the state of the art. It continues with the PV power generator modeling, which will define the amount of energy that can be supplied to the micro grid. It follows with the training phase of the NNF, it is used a three years dataset (2010-2013) measured by an in situ weather station. The collected variables are time (hour, day, and month) pressure, solar irradiance and temperature. Finally, the model is simulated step by step by MATLAB / Simulink, which let to obtain behavior graphs and thus results analysis and conclusions remarks.

Keywords: Microgrid, Neural Network, Renewable Energy, Photovoltaic System

INTRODUCTION

Current methods for energy production are not sustainable due to environmental reasons and the lack of responsible use of resources. Therefore, demand for renewable energy, smart electrification and rational use of available energy are important factors that will provide answers to the global energy challenge (James et al, 2009). Industry nowadays is mainly dependent on energy generated from fossil fuels, hydroelectric processes or nuclear reactions, with centralized large-scale distribution systems where efficiency loss can be up to 69%. This engineering challenge is to be solved with non-polluting decentralized generation of renewable energy and innovating concepts such as “smart grid". A smart grid generally refers to a group of people that use technology, control systems and remote computer automation to manage the electricity supply from the public grid, along with renewable energy sources. Implementation of this concept can be found today in systems integrating power plants, wind farms and end consumers [1] [17], providing a foundation framework for future sustainable energy systems and allowing integration of large amounts of renewable energy with improved reliability, quality and supply security. Thus, given the former advantages and breakthroughs in renewable energy generation, it is necessary to analyze how energy should be used in a DC micro grid that integrates renewable energy sources, where power generation is used to supply user needs without requiring transformation from direct current (DC) to alternating current (AC) and vice versa [4], [14].

Nevertheless, 66% of Colombian territory is not connected to the National Grid. These regions are called Non-Interconnected Zones (NIZ) and their energy requirements are covered using traditional fuels (such as small hydroelectric projects, diesel or biomass) or from a few Renewable Energy Sources (RES) projects, but the lack of available energy or low quality of supply service in these regions are still caused by social and economic constraints. On the other hand, the energy generation industry has been based on free market policies since 1994, which have caused several RES projects being discarded due to a lack of economic incentives. Despite the aforementioned limitations, the Institute for the Promotion of Energy Services (IPSE, by the acronym in Spanish) is in charge of creating RES projects in Non-Interconnected Zones; its Financial Office (Financial Support Fund for the Electrification of NIZ, FANZI,

by the acronym in Spanish) has allocated more than US$85 million to this kind of projects since 2003 [21].

In this context, it is vital to perform Innovation and Technological Development projects related with emerging technologies in such a manner that they achieve greater electrical energy efficiency and lower (or lack of) polluting emissions. Therefore, the work presented in this paper is part of a larger research project focused on managing energy generated by different devices, such as photovoltaic cells and wind turbines. Said management is crucial towards generating cost savings due to lesser dependency on the public energy grid and higher use of available renewable energy. In engineering terms this management will be performed by a Model Predictive Controller (MPC) (to be implemented in future works) [25], [9], [5], [18], [16], [15], [13], where predicting the state of available resources is required as a design parameter. Prediction theory associated to this type of controllers highlights that, though available algorithms are imperfect, they are applied with acceptable levels of uncertainty. One of the most largely used methods for forecast of meteorological data is the NNF Curve [2], [8], [19], [3]. A thorough revision of previous work evidences greater performance obtained using a NNF curve when compared to other prediction methods such as NARX, NAR and ARMAX [6].

The implemented micro-grid has two different types of power generators and one energy storage device, the proposed prototype is shown in Figure 1.

The system has a set of twelve 300 W PV modules (Bosh c- Si-M60 - M260), a generic low-speed wind turbine, a battery bank and the corresponding converters. The micro grid is used to light two tennis courts at the university sports complex located in Cajicá's Campus; its characteristic weather is mild and warm, with regular raining even during the driest month of the year. The climate classification according to Köppen-Geiger is Subtropical with Oceanic Station, Cfb and the average annual temperature is 14.0 °C with 830 mm rainfall [17].

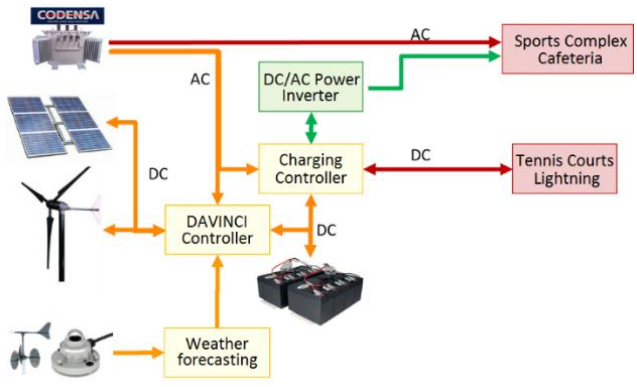

Figure 1. Prototype and Model System.

The structure of this article is given as follows: First, a photovoltaic model is formulated. Then, the NNF with meteorological data is implemented. Finally, prediction data regarding solar irradiance is obtained, as well as the corresponding current that will be generated according to said prediction.

PHOTOVOLTAIC MODEL

Considering the micro-grid structure given in Figure 1, we establish the PV model to know the energy produced by PV and the battery load.

The PV is represented as an electrical circuit that provides current I_{ph} from sunlight (photocurrent), this current source is connected to a diode and a resistor R_p in parallel and both interconnected in series to a resistor R_s which finally generates the difference potential V, as shown in Figure 2. [7], [10].

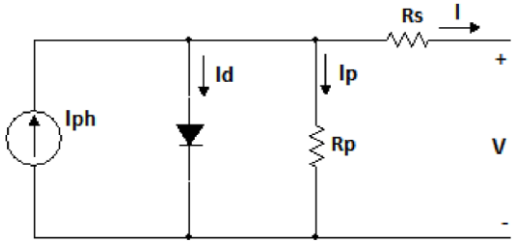

Figure 2. PV simplified Model.

This is a nonlinear model that involves several parameters classified in three groups: those provided by the manufacturer, the electrochemical constants that can be assumed according to electromechanical and weather conditions, and the ones that can be calculated.

The idea of this work is to obtain a model that can be as precise as the experimental measurements, but still maintaining its ease in terms of required computations. Thus, one of the developed model's advantages is its ability to operate with few parameters in the same way as a real system. This feature makes it ideal for use within an integrated energy system, even though it does not take power losses into account.

According to the simplified model panel shown in Figure 2, the equation that defines the PV model dynamics in terms of an output current can obtained via Kirchhoff's current law, as shown in Eq. (1):

$$I = I_{ph} - I_d - I_p \qquad 1)$$

The current through the parallel resistor can be defined by Ohm' law Eq (2) and the photocurrent as a relative value of the reference and the variation produced by the cells' temperature, amplified by the irradiance, Eq. (3):

$$I_p = \frac{V + R_s \cdot I}{R_p} \qquad (2)$$

$$I_{ph} = \frac{G}{G_{ref}} \left(I_{ph,ref} + \mu_{sc} \cdot \Delta T \right) \qquad (3)$$

Where V is the voltage imposed on the diode, G is the irradiance, G_{ref} is the solar irradiance in Standard Test Conditions (STC), T_c is the cells' temperature, thus $\Delta T = T_c -$

$T_{c,ref}$ ($T_{c,ref} = 298K$) and μ_{sc} is the temperature coefficient for a short-circuit current (given by the manufacturer).

The Eq. (4) is based in the ideal Shockley diode equation, which gives the $I - V$ characteristic in either forward or reverse configuration.

$$I_d = I_o \left[\exp\left(\frac{V + I \cdot R_s}{a}\right) - 1 \right] \rightarrow a = A \cdot N_s \cdot V_T \quad (4)$$

A is the ideality factor for monocrystalline silicon cells, N_s is the number of photovoltaic cells connected in series and V_T is the thermal factor, defined in the Eq. (5) in terms of the Boltzmann constant k, the electron charge q and the actual cells temperature T_c. The Eq. (6) defines the reverse saturation or the leakage current I_o.

$$V_T = k \cdot T_c / q \quad (5)$$

$$I_o = I_{o.ref} \left(\frac{T_c}{T_{c,ref}}\right)^3 \exp\left[\left(\frac{q\varepsilon_G}{Ak}\right) \left(\frac{1}{T_{c,ref}} - \frac{1}{T_c}\right) \right] \quad (6)$$

The Eq. (6) depends of the electrochemical constants, including the material (silicon) band gap energy ε_G, as well as the temperature and the leakage reference current on $I_{o,ref}$, that is defined in the Eq. (7) in terms of open circuit voltage ($I = 0, V = V_{oc}$) and the short circuit current ($V = 0, I = I_{sc}$) in STC.

$$I_{o.ref} = I_{sc}\, exp\left(-\frac{V_{oc.ref}}{a}\right) \quad (7)$$

Therefore, the Eqs.(1), (2), (3) and (4) are used to obtain the PV output current using the parameters in the table 1. The PV parameters (defined by the manufacturer) were obtained from the silicon cell's reference (Bosch c-Si M60-M260). P_{mp} , I_{mp} y V_{mp} are maximum power, current for maximum power and voltage for maximum power respectively (tested by the PV manufacturer).

As previously stated, the model consists of resistance R_p and R_s as is shown in the Eq. (2), the parallel resistor can t obtained using Eq. (8).

$$R_p = \frac{V_{mp} + I_{mp} \cdot R_s}{I_{sc.ref} \cdot m - \frac{P_{mp}}{V_{mp}}} \quad (8)$$

$$m = 1 - \exp\left[\frac{V_{mp} + R_s\, I_{mp} - V_{oc}}{a}\right] + \exp\left(-\frac{V_{oc}}{a}\right) \quad (9)$$

Several values of R_s were proposed to obtain the most appropriate values of R_p and reach the maximum power established by the manufacturer. Figure 3 shows the $I - V$ model behavior, presenting different values of R_s.

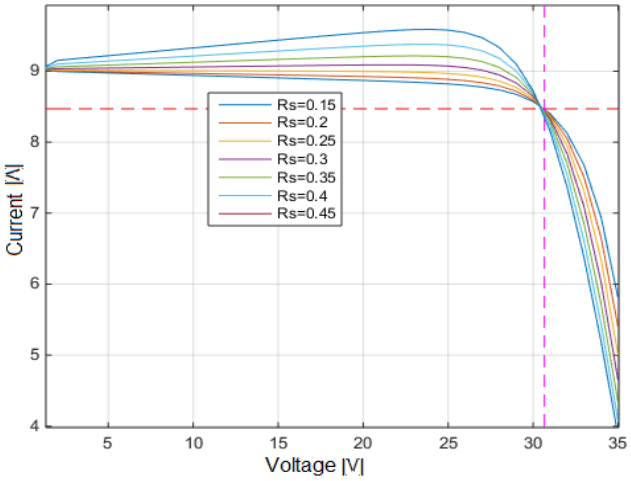

Figure 3. PV Simulation with different values of R_s.

This graphic allows selection of $R_s = 0{,}25\Omega$, thus obtaining the current and voltage lines (broken line with maximum values of V_{mp} and I_{mp}, as is shown in

The block diagram shown in Figure 4 was implemented in MATLAB-Simulink and represented in the equations of this section.

Once the best values of R_p and R_s were chosen, the simulation was compared with the defined values of P_{mp}, V_{mp} and I_{mp} given by the manufacturer. The results were validated and are shown in the Figure 5.

Table 1).

The block diagram shown in Figure 4 was implemented in MATLAB-Simulink and represented in the equations of this section.

Once the best values of R_p and R_s were chosen, the simulation was compared with the defined values of P_{mp}, V_{mp} and I_{mp} given by the manufacturer. The results were validated and are shown in the Figure 5.

Table 1: Photovoltaic parameters.

DEVICE PARAMETERS		STC CONSTANTS	
PARAMETER	VALUE	PARAMETER	VALUE
N_S	60	k	$1{,}381 \cdot 10^{-23}$
P_{mp}	260	q	$1{,}602 \cdot 10^{-19}$
V_{mp}	30,71	G_{ref}	1000

I_{mp}	8,47	$T_{c.ref}$	298
I_{sc}	9,02	Variables to obtain	
V_{sc}	38,1	R_s	R_p
μ_{sc}	3,1	I_{pk}	I_o
A	1,2	Inputs	
ε_G	1,12	G	T_c

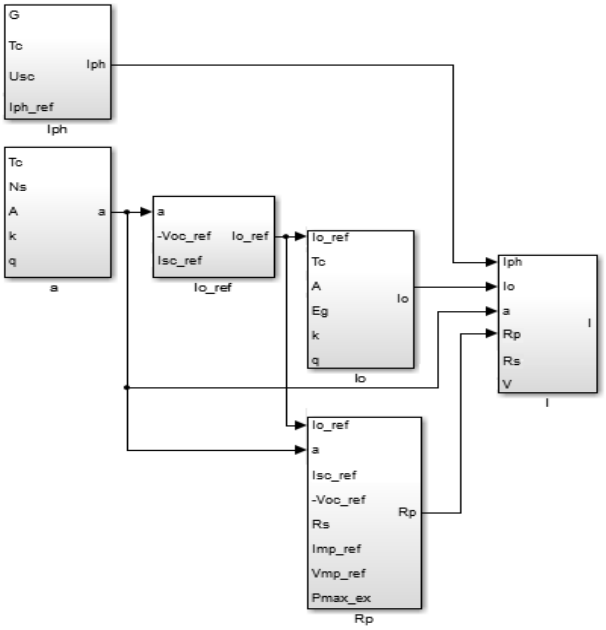

Figure 4. PV block diagram.

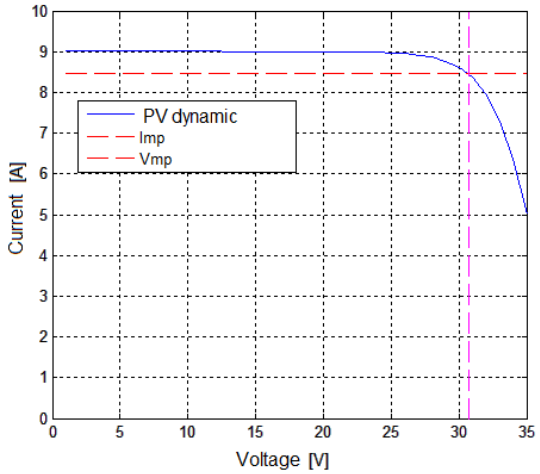

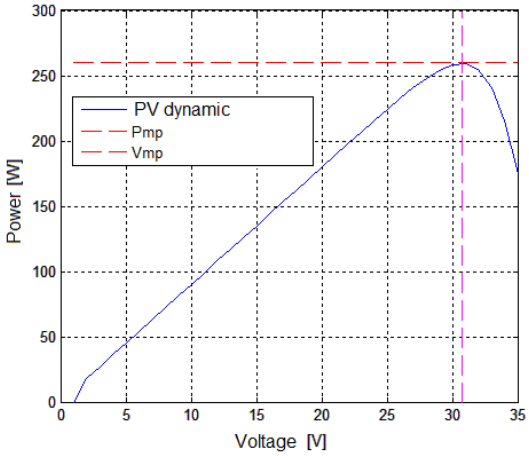

Figure 5. V-P Simulation using V-I values.

NNF MODEL

This section shows the implementation of a neural network that allows prediction of the energy supplied by the PV from meteorological data. Data inputs for the neural network include day (D), month (M), hour (H), atmosphere pressure (AP), solar irradiance (SR) and environmental temperature (ET), taken from the CAR database from 2010 to 2013. The purpose of this implementation is to estimate the amount of solar irradiance and the energy that can be provided to the batteries one hour beforehand. The implemented model is based on a Neural Network/Curve Fitting estimation, a special set of algorithms for function monitoring and/or adjustment; this becomes an advantage given its ease of adaptation to any practical function.

The Eq. (9) describes the mathematical model used in the NNF.

$$y(t) = f(\, w_1\, x(t-1) + b_1 \ldots w_n\, x(t-n) + b_n) \qquad (9)$$

Where $x(t)$ and $y(t)$ are the inputs and outputs respectively, f is a nonlinear function, w_n is the polynomial's weight coefficient and b_n is the neural network's activation bias. The neural network's structure is as follows: a hidden layer with 10 neurons using a sigmoid activation function and a single-neuron output layer using an identity activation function, as is shown in

Figure **6**.

The function's approximation is the setting that is made in a Neural Network in order to deduce the relationship between the input and output (through supervised learning), using a set of input-output data. Once a relationship between the input and output has been modeled with the necessary precision, it can be used for several tasks, such as function prediction, approximation, and optimization [20].

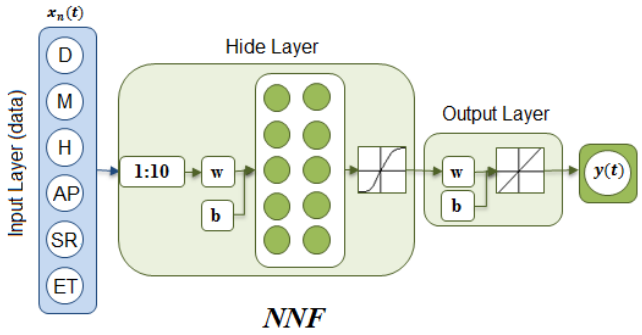

Figure 6. NNF Structure.

In the Figure 7, values of R from the regression made by the Neural Network are shown. In general, this graphic allows validation of neural efficiency and finding a relationship between the Neural Network output and the training targets.

The perfect data adjustment should be a 45 degrees line (one-to-one correlation), where the number of network outputs is equal to the number of targets. In this issue, the adjustment is reasonably good for all data sets, with R values of 0,92 or higher. The R is determined through Eq. (10), where y_{pt} y y_t represent the prediction and measurement test values, respectively. y_{tr} is the training value average [23].

$$R = \sqrt{1 - \left(\frac{\Sigma[y_{pt} - y_t]^2}{\Sigma_j[y_t - \bar{y}_{tr}]^2}\right)} \qquad (10)$$

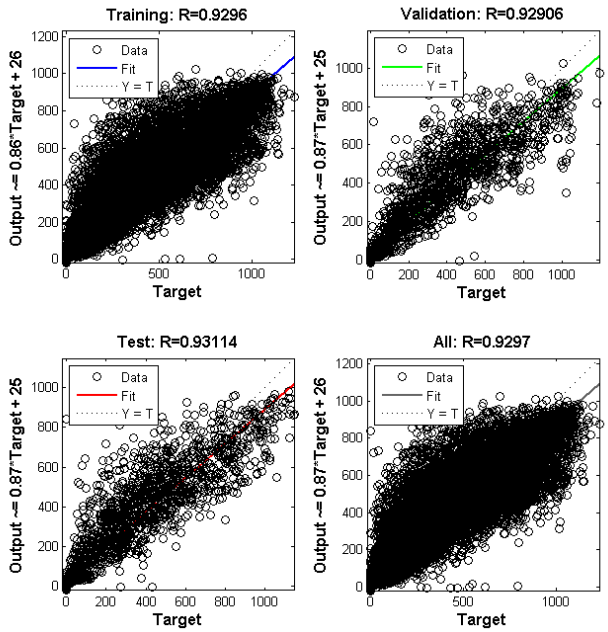

Figure 7. Neural Network performance.

RESULTS

The following section shows implementation results for the predictive model, as well as how it can be used to estimate irradiance values after its training. Figure 8 shows how the neural network achieves the predicted solar irradiance measurement in a sunny day with clouds in the midday.

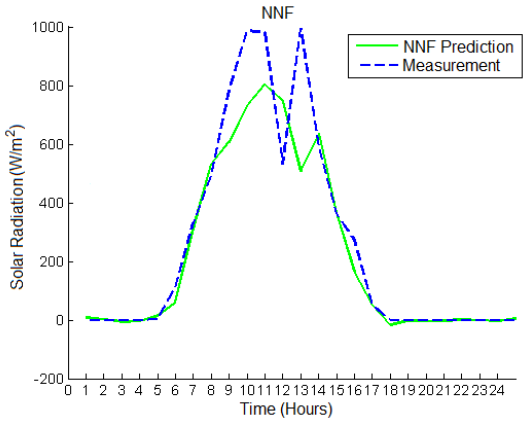

Figure 8. Comparison of measurement and prediction of solar radiation.

In Figure 8 it is seen that the neural network can make a correct prediction, given that it appropriately follows the measurement curve. The approximation can be validated by means of the mean and asymmetry relation for each graphic. The asymmetry relation is determined using the Fisher coefficient Eq. (11) which shows the asymmetry level between two graphics [24].

$$g = \frac{(1/n) \cdot \sum (x_i - x_m)^3 \cdot n_i}{((1/n) \cdot \sum (x_i - x_m)^2 \cdot n_i)^{3/2}} \qquad (11)$$

Its results can be analyzed as follows:

- $g_1 = 0$ (symmetrical distribution; same value concentration on both sides of the mean value)
- $g_1 > 0$ (asymmetrical positive distribution; higher value concentration to the right of the mean value)
- $g_1 < 0$ (asymmetrical negative distribution; higher value concentration to the left of the mean value)

Other methods used to validate the measured model's precision are the Mean Squared Error (MSE), Mean Absolute Error (MAE), Sum of Squared Error (MSE) and Sum of Absolute Error (MAE), which measure the average of the square or the absolute value of the errors (subtractions) [12], according to Eqs. (12), (13), (14) and (15).

$$\text{MSE} = \frac{1}{\text{N}} \sum_{\text{i}=1}^{\text{N}} [\,\text{y}_\text{i} - \hat{\text{y}}_\text{i}\,]^2 \qquad (12)$$

$$\text{MAE} = \frac{1}{\text{N}} \sum_{\text{i}=1}^{\text{N}} [\,\text{y}_\text{i} - \hat{\text{y}}_\text{i}\,] \qquad (13)$$

$$SSE = \sum_{i=1}^{N} [\, y_i - \hat{y}_i \,]^2 \qquad (14)$$

$$SAE = \sum_{i=1}^{N} [\, y_i - \hat{y}_i \,] \qquad (15)$$

Where N is the total number of data, y_i is an array of target values and $\hat{y}_i$ is the corresponding estimated values [22]. Most rules define the precision of the estimation as a difference between real and estimated values. These Values are shown in Table 2.

Table 2: Prediction Data.

MEASUREMENT		NNF PREDICTION	
PARAMETER	VALUE	PARAMETER	VALUE
Average	2,32	Average	2.08
Error	260	10053,4	
	30,71	$3{,}112 \cdot 10^8$	
	8,47	1,635	
	9,02	54,285	
Fisher Coefficient		0,15	

The Fisher coefficient is 0,15, showing that the sample has an asymmetrical positive distribution. Both predicted and measured solar irradiance data are inputs for the mathematical PV model to know the amount of power which would be available to charge the batteries.

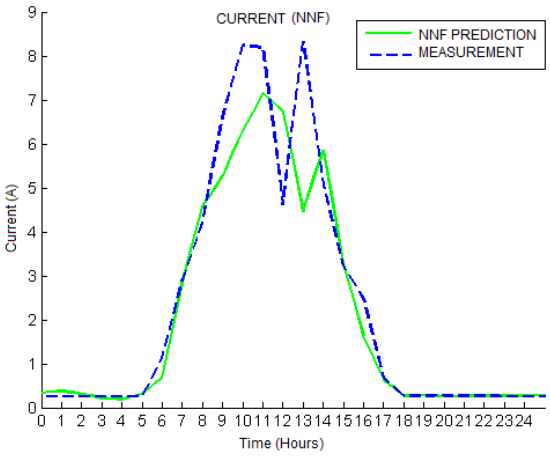

Figure 9. Comparison of measurement vs current prediction.

Solar prediction irradiance data is entered into the system (solar panel and battery) as shown in Figure 10 to determine if the system can withstand a 20A load and in turn charge a bank of twenty-four 2V-1000A batteries.

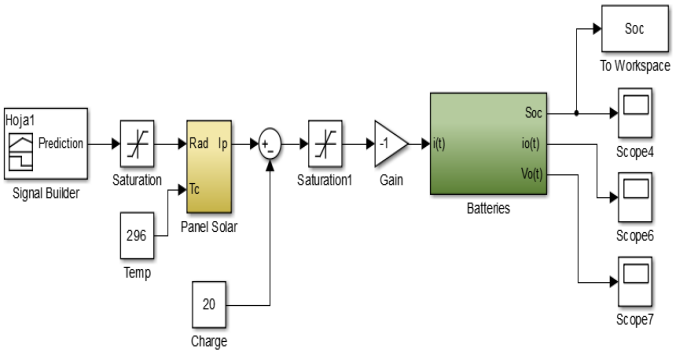

Figure 10. Battery and Solar Panel system.

The SOC of the battery bank is shown in Figure 11. This graph shows that starting from 60%, batteries reach 91,2% charge. This case is considered critical because it starts from the lowest charge level. If the energy demand exceeds its established limit, or if the solar irradiance is lower than shown, the system will use the micro-grid to charge the batteries.

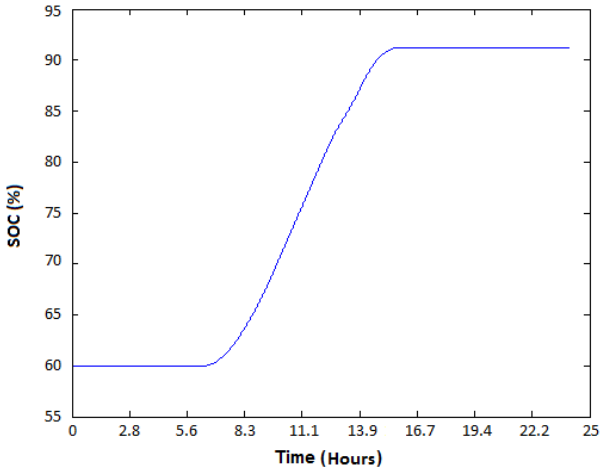

Figure 11. Level of battery charge.

CONCLUSIONS

The obtained PV model presents a nonlinear current equation in terms of the desired output voltage and two meteorological variables, irradiance and temperature. The diode's exponential dynamics introduce this nonlinearity. Therefore, the $I - V$ table shows a decreasing curve that begins when the PV is short-circuited ($V = 0, I = I_{sc}$) and finishes when the PV is open circuit ($I = 0, V = V_{oc}$). Besides, the PV works with a nominal voltage of $V = 24V$ with a maximum power point when $= V_{mp} = 30{,}71V$; this translates to a current of $I = I_{mp} = 9{,}02A$ and therefore a power of $P = P_{mp} = 260W$ in accordance with the parameters given by the manufacturer.

Adjustment of data generated by the grid has a high degree of correspondence between the target data and the output (for all data sets), with a R value equal to 0,92. This indicates that the prediction will can follow the real signal maintaining a low prediction error.

Solar irradiance prediction results cannot fully follow the measurement signal due to configuration limitations in the MATLAB toolbox. One possibility for improvement is increasing the number of hidden layers within the neural network.

System simulation tests were performed assuming an initial charge state of 60% in the batteries and current values defined by the prediction of solar irradiance in a average day, with results indicating that the system can fully charge the batteries and withstand the established load.

As future work, a controller based on predicted data will be developed and implemented, which will be in charge of managing the micro-grid's energy supply. Said management will depend on resource estimation: calculating which energy supply generates the highest amount of charge to the batteries in each time space and avoiding use of the local power supply whenever possible.

ACKNOWLEDGEMENT

This work was financially supported by Nueva Granada Militar University's Research Vicepresidency. Funding was provided through the ING-1577 research project, titled "Development, automation and control of a hybrid renewable resources plant" (2014-2015).

REFERENCES

[1] Almonacid, F. Fernández, E. Mallick, T. and Pérez-Higueras, P. "High concentrator photovoltaic module simulation by neuronal networks using spectrally corrected direct normal irradiance and cell temperature," Energy, vol. 84, pp. 336–343,2015.[Online].Available:http://linkinghub.elsevier.com/retrieve/pii/S0360544215002832.

[2] Álvarez Bel, C. Escrivá-Escrivá, G. and Alcázar-Ortega, M. "Renewable generation and demand response integration in micro-grids: Deve- lopment of a new energy management and control system," Energy Efficiency, vol. 6, no. 4, pp. 695–706, 2013.

[3] Arnold, M. and Andersson, G. "Model Predictive Control of Energy Sto- rage including Uncertain Forecasts," 17th Power Systems Computation Conference, pp. 1–7, 2011.

[4] Bellia, H. Youcef, R. and Fatima, M. "A detailed modeling of photovoltaic module using MATLAB," NRIAG Journal of Astronomy and Geophysics, vol. 3, no. 1, pp. 53–61, Jun.2014.[Online].Available:http://www.sciencedirect.com/science/article/pii/S2090997714000182.

[5] Braik, M. Sheta, A. and Arieqat, A. "A Comparison between GAs and PSO in Training ANN to Model the TE Chemical Process Reactor," Proceedings of the AISB 2008 Symposium on Swarm Intelligence Algo- rithms and Applications, pp. 24–31, 2008.

[6] Bordons, C. García-Torres, F. and Valverde, L. "Gestión Óptima de la Energía en Microrredes con Generación Renovable," Revista Iberoamericana de Automática e Informática Industrial RIAI, vol. 12, no. 2, pp. 117–132, 2015. [Online]. Available: http://linkinghub.elsevier.com/retrieve/pii/S1697791215000023

[7] Camacho, E. F. and Bordons, C. "Model Predictive control," ser. Advanced Textbooks in Control and Signal Processing. London: Springer London, 2007. [Online]. Available: http://link.springer.com/10.1007/978-0-85729-398-5

[8] Chuanchuan, C. Jun, Z. and Panpan, J. "Multi-agent system applied to energy management system for renewable energy micro-grid," 2013 5th International Conference on Power Electronics Systems and Applications(PESA), Hong Kong, 2013, pp. 1-6. doi: 10.1109/PESA.2013.6828222

[9] Cobb, G. W. Moore, D. S. Cobb, G. W. and Moore, D. S. "Mathematics, Statistics and Teaching," vol. 104, no. 9, pp. 801–823, 2015.

[10] García-Domingo, B. Aguilera, J. De la Casa, J. and Fuentes, M. "Modelling the influence of atmospheric conditions on the outdoor real performance of a CPV (Concentrated Photovoltaic) module," Energy, vol. 70, no. 2014, pp. 239–250,2014.[Online].Available:http://dx.doi.org/10.1016/j.energy.2014.03.119.

[11] Garcia, F. and Bordons, C. "Regulation service for the short-term management of renewable energy microgrids with hybrid storage using Model Predictive Control," IECON Proceedings (Industrial Electronics Conference), pp. 7962–7967, 2013.

[12] Gao, Yue-Ming and Du, Min "Wavelet neural network based calibration curve fitting in the quantitative assay," 2007 International Conference on Wavelet Analysis and Pattern Recognition, Beijing,. 2007, pp. 793-797. doi: 10.1109/ICWAPR.2007.4420777.

[13] Gridwise Alliance, "The future of the Grid, Evolving to Meet America's Needs," 2014. Wiley, Green Extraction of Natural Products: Theory and Practice. Wiley, 2015.[Online].Available:https://books.google.com/books?id=MRB9BgAAQBAJ&pgis=1

[14] Ishaque, K. Salam, Z. Taheri, H. and Syafaruddin, "Modeling and simulation of photovoltaic (PV) system during partial shading based on a two-diode model," Simulation Modelling Practice and Theory, vol. 19, no. 7, pp. 1613–1626,2011.[Online].Available:http://dx.doi.org/10.1016/j.simpat.2011.04.005.

[15] James F. Manwell, Jon G. McGowan, Anthony L. Rogers, "Wind Energy Explained, 2009. Wiley. ISBN: 978-0-470-01500-1

[16] Luo, H. Liu, D. and Huang, Y. "Artificial neural network modeling of algal bloom in Xiangxi Bay of Three

Gorges Reservoir," 2010 International Conference on Intelligent Control and Information Processing, Dalian, 2010, pp. 645-647. doi: 10.1109/ICICIP.2010.5564258

[17] Mauledoux, M. Caldas, O. I. and Mejía-Ruda, E. "Comparative Study of Various Models to Estimate Hourly Solar Irradiance: Application for Performance Analysis of a Renewable Energy DC-Micro Grid," Applied Mechanics and Materials, vol. 700, pp. 7–11, 2014. [Online]. Available: http://www.scientific.net/AMM.700.7.

[18] Pelland, S. Galanis, G. and Kallos, G. "Solar and photovoltaic forecasting through post-processing of the Global Environmental Multiscale numerical weather prediction model," Progress in Photovoltaics: Research and Applications, vol. 21, no. 3, pp. 284–296, May 2013. [Online]. Available: http://www.readcube.com/articles/10.1002%2Fpip.1180?r3_referer=wol&tracking_action=review_click&show_checkout=1&purchase_referrer=onlinelibrary.wiley.com&purchase_site_license=LICENSE_DENIED

[19] Peña Cabra, I.A "Renewable Energy Sources for the Non- Intercon- nected Zones in Colombia," no. April, pp. 1–43, 2009.

[20] Rawlings, J. B. and Muske, K. R. "Stability of constrained receding horizon control," IEEE Transactions on Automatic Control, vol. 38, no. 10, pp. 1512–1516, 1993.

[21] Singh V. P., Vivek Vijay, M. S. Bhatt, and Chaturvedi D. K., "Generali- zed Neural Network Methodology For Short-Term Solar Power Forecas- ting," 13th IEEE Envieronment and electrical engineering International Conference Poland(EEEIC-2013), 2013.

[22] Tarade, R. S. and Katti, P. K."A comparative analysis for wind speed prediction," 2011 International Conference on Energy, Automation and Signal, pp. 1–6, 2011.

[23] Tsoeu, M. S. and Koetje, T. "Unconstrained MPC tuning for prediction accuracy in Networked Control Systems," 2011 International Conferen- ce on Networking, Sensing and Control, ICNSC 2011, no. April, pp.474–479, 2011.

[24] Valverde, L. Bordons, C. and Rosa, F. "Power Management using Model Predictive Control in a hydrogen-based microgrid," IECON 2012 - 38th Annual Conference on IEEE Industrial Electronics Society, pp. 5669–5676, 2012.

[25] Yadav, A. K. and Ann, S. "Artificial Neural Network based Prediction of Solar Radiation for Indian Stations," vol. 50, no. 9, pp. 1–4, 2012.